Periodic Binary Si:Ti, Si:Al Mixed Macroporous Oxides with Ultrahigh Heteroatom Loading: A Facile Sol−Gel Approach

Steven M. Hant,[†] George S. Attard,[†] Rodney Riddle,[‡] and Kevin M. Ryan*,[‡]

School of Chemistry, University of Southampton, Highfield, Southampton, United Kingdom, SO17 1BJ, and Merck Chemicals, Ltd., Chilworth Technical Centre, Chilworth, Southampton, United Kingdom, SO16 7QD

Received October 5, 2004. Revised Manuscript Received January 11, 2005

Highly ordered macroporous mixed metal oxides were prepared with very high mixed metal ratios using an optimized silicon alkoxide prehydrolysis process. The homogeneous solutions completely filled the interstitial voids in polymethyl methacrylate artificial opal templates. Subsequent template removal resulted in highly ordered aluminosilicate and titanosilicate inverse opal pore networks. The optimized process allowed the fabrication of periodic binary metal oxide frameworks with 2:1 Si:Al loadings and 1:1 Si:Ti loadings. The mixed metal oxides did not show any phase segregation during high-temperature template removal as evidenced by X-ray diffraction, energy-dispersive X-ray analysis, and Fourier-transform IR spectroscopy. The as-formed macroporous metal oxides demonstrate excellent substrate adherence and mechanical stability and showed refractive index modulation in direct relation to the silicon/heterometal ratio in the precursor sol.

Introduction

Periodic macroporous materials are of continued interest for adsorption, separation, catalysis, and molecular hosting of organic, inorganic, and biological systems >50 nm.[1−8] The sub-micrometer structure further allows Bragg diffraction of visible light, producing vivid optical color shifts suitable for pigment applications in the less-ordered and optoelectronics in the most-ordered systems.[9−11]

Three-dimensional ordered macroporous materials with periodicities in the sub-micrometer size range are more difficult to fabricate than their microporous (<2 nm) or mesoporous analogues (2−50 nm).[12] Techniques such as emulsion templating, rod-coil block copolymer self-assembly, and solvent evaporation have resulted in foamlike materials with minimal structural order.[13−16] The most successful route employs ordered arrays of sub-micrometer spheres as inverse templates.[17] Infiltration of the interstitial voids with materials, using chemical vapor deposition (CVD), electrodeposition, or sol−gel deposition, followed by template removal leaves a highly ordered interconnected porous spheroid matrix.[18] The resultant macroporous material replicates point, line, and planar defects present in the original packed spheres with further defects arising from incomplete void filling and cracking during template removal.[19] Defects in artificial opal synthesis can be minimized by using monodisperse colloidal spheres and slow gravity-dependent packing mechanisms. However, defects arising during material infiltration and template burnoff are more difficult to control.

Sol−gel-templated inverse opals of silica, titania, and alumina are widely reported.[20,21] Recently, Becheger et al.[22] described the consecutive deposition of ZrO_2, TiO_2, and Al_2O_3 to form macroporous oxides with multilayered pore walls. However, the incorporation of mixed metal oxide infiltrates has not been significantly reported. Mixed metal oxide macroporous composites of silicon/aluminum and silicon/titanium are of potential interest for catalytic and ion exchange applications.[23] Porous titanosilicates have found application as epoxidation catalysts of long-chain olefins and, in more recent studies, as photocatalysts for the decomposition of organic matter.[8,24,25] The band-gap structure of titania

* To whom correspondence should be addressed. E-mail: kevin.ryan@merckchem.co.uk, k.ryan@ifnano.com.
[†] University of Southampton.
[‡] Merck Chemicals, Ltd.

(1) Yang, Y.; Guo, Y.; Hu, C.; Wang, E. *Appl. Catal., A* **2003**, *252*, 305.
(2) Johnson, B. J. S.; Stein, A. *Inorg. Chem.* **2001**, *40*, 801.
(3) Farrusseng, D.; Julbe, A.; Guizard, C. *Sep. Pur. Technol.* **2001**, *25*, 137.
(4) Choudhary, V. R.; Mamman, A. S.; Uphade, B. S.; Babcock, R. E. *ACS Symp. Ser.* **2002**, *809*, 224.
(5) Yabuki, M.; Takahashi, R.; Sato, S.; Sodesawa, T.; Ogura, K. *Phys. Chem. Chem. Phys.* **2002**, *4*, 4830.
(6) Gille, W.; Enke, D.; Janowski, F.; Hahn, T. *Catal. Lett.* **2004**, *93*, 13.
(7) Nowak, I. *Colloids Surf., A* **2004**, *241*, 103.
(8) Rubio, F.; Rubio, J.; Oteo, J. L. *J. Sol−Gel Sci. Technol.* **2000**, *18*, 105.
(9) Jiang, M.; Bertone, J. F.; Hwang, K. S.; Colvin, V. L. *Chem. Mater.* **1999**, *11*, 2132.
(10) Schroden, R. C.; Al-Daous, M.; Blanford, C. F.; Stein, A. *Chem. Mater.* **2002**, *14*, 3305.
(11) Ni, P.; Dong, P.; Cheng, B.; Li, X.; Zhang, D. *Adv. Mater.* **2001**, *13*, 437.
(12) Soller-Illia, G. J. A. A.; Sanchez, C.; Lebeau, B.; Patarin, J. *Chem. Rev.* **2002**, *102*, 4093.
(13) Imhof, A.; Pine, D. J. *Nature* **1997**, *389*, 948.
(14) Imhof, A.; Pine, D. J. *Adv. Mater.* **1998**, *10*, 697.
(15) Jenekhe, S. A. *Science* **1998**, *279*, 1903.
(16) Widawski, G.; Rawiso, M.; Francois, B. *Nature* **1994**, *369*, 387.
(17) Velev, O. D.; Jede, T. A.; Lobo, R. F.; Lenhoff, A. M. *Nature* **1997**, *389*, 447.
(18) Xia, Y.; Gates, B.; Yin, Y.; Lu, Y. *Adv. Mater.* **2000**, *12*, 693.
(19) Wong, S.; Kitaev, V.; Ozin, G. A. *J. Am. Chem. Soc.* **2003**, *125*, 15589.
(20) Jiang, P.; Cizeron, J.; Bertone, J. F.; Colvin, V. L. *J. Am. Chem. Soc.* **1999**, *121*, 7957.
(21) Turner, M. E.; Trentler, T. J.; Colvin, V. L. *Adv. Mater.* **2001**, *13*, 180.
(22) Becheger, L.; Vos, W. L. *Chem. Mater.* **2004**, in press.
(23) Dirken, P. J.; Smith, M. E.; Whitfield, H. J. *J. Phys. Chem. B* **1995**, *99*, 395.

10.1021/cm0482582 CCC: $30.25
Published on Web 02/22/2005

(rutile phase, band gap of 3.2 eV), is an effective absorber of UV light, producing electron−hole pairs for the oxidation of adsorbed donor molecules and the reduction of adsorbed acceptor molecules, respectively.[26] Porous aluminosilicate frameworks have found a niche application as solid-acid catalysts. Tetrahedrally coordinated aluminum ions, at the pore walls, function as Bronsted acid sites ideal for catalytic cracking of fuel oils.[27,28] In addition, macroporous alumina membranes have demonstrated strong potential for the selective oxidation of alkane gases.[29]

Achieving high heteroatom aluminum and titanium loadings via the sol−gel route has proven difficult. The problem arises from incompatibility in hydrolysis rates of alkoxides of silicon to those of aluminum or titanium. The faster hydrolyzing aluminum alkoxide and titanium alkoxide species favor dimerization over reaction with silicon alkoxide, resulting in precipitation of aluminum- or titanium-rich compounds. A review by Davis and Liu[30] described the formation of sol−gel precursors with molar ratios of Si:Ti 1:1 using a silicon alkoxide prehydrolysis technique in the presence of titanium isopropropoxide. However, the introduction of ordered porosity was found to greatly reduce the attainable heteroatom incorporation. In particular, titanium loading in porous silica films were reported by Ogawa et al. with molar ratios Si:Ti, 50:1 using a solvent evaporation technique.[31] Loadings of 20% (5:1 Si:Ti) have been obtained in mesoporous silica through selective complexation of titanium alkoxide species to reduce the active sites for hydrolysis.[24] However, the presence of complexing species also restricts the condensation process, resulting in films with poor mechanical and thermal stability. The limit for titania loading in ordered macroporous silica is approximately 25%, requiring sterically hindered titanium alkoxides to slow the initial hydrolysis rates.[32] Similarly, alumina loading in macroporous and mesoporous oxides is currently limited to 20%.[28,33] Ordered porous oxides produced using these methods are typically inhomogeneous and suffer from heterometal leaching at temperatures required for template removal. To date, stable macroporous silica films with high (>25%) loadings of aluminum or titanium have not been reported.

In this paper, we report an optimization of the silicon alkoxide prehydrolysis technique described independently by Yoldas,[34] Best,[35] and Schraml-Marth[36] to allow the direct formation of highly ordered mixed metal oxide macroporous materials with Si:Al ratios of 2:1 (33% loading) and Si:Ti ratios of 1:1 (50% loading), respectively. The optimized solutions use very low concentrations of acid catalyst, precisely controlled prehydrolysis temperatures, and judicious addition of the titanium alkoxide in the presence of specific silicon intermediates. The solutions have excellent wetting characteristics allowing infiltration of face-centered cubic (fcc) packed arrays of polymethyl methacrylate (PMMA) spheres and complete filling of interstitial voids in a single step. The resultant macroporous metal oxides are defect free over large areas and show no evidence of metal leaching during the template removal process.

Experimental Section

Materials. PMMA spheres with a diameter of 365 ± 10 nm were obtained from Merck Chemicals, Ltd., as a 14 wt % suspension in water. Tetraethyl orthosilicate (TEOS, $Si(OC_2H_5)_4$), aluminum tri-*sec*-butoxide ($((C_2H_5CH(CH_3)O)_3Al$), and titanium(IV) ethoxide ($Ti(OC_2H_5)_4$) were purchased from Aldrich. Dilute acidic solutions were prepared from 1 M HCl solutions re-dispersed in deionized water. Pure-grade (98%) ethanol was obtained from VWR. Glass slides were obtained from Menzel-Glaser. Teflon rings with an internal diameter of 10 mm, external diameter of 20 mm, and a height of 10 mm were constructed at the University of Southampton laboratories.

Assembly of the Colloidal Templates. The colloidal crystal templates were assembled by a gravity sedimentation method. Microscope slides were precleaned by sequential sonication in water, acetone, isopropyl alcohol, and chloroform before a Teflon ring was attached using a ring of double-sided tape. The monodisperse suspension (0.5 mL) of PMMA spheres diluted with water to 1 wt % was confined within the Teflon ring. The assembly was placed in a saturated humidity chamber for 2−3 days before allowing the solvent to evaporate at 3 °C over 5 days. The Teflon ring was subsequently removed, exposing a circular iridescent packed array of PMMA spheres on the substrate. This approach formed uniform films of ca. 40 μm thickness.

Preparation of Aluminosilicate and Titanosilicate Sol−Gel Precursors. Aluminosilicate and titanosilicate sol−gel precursor solutions were prepared by the optimized prehydrolysis method recently described by Ryan et al.[37] for the production of mesoporous thin films. TEOS (Aldrich, 10 g), ethanol (5.4 g), and HCl (0.8 mL, 0.1 M) were mixed and stirred at 37 °C for 10 min to prehyrolyse the silica precursor. The solution was cooled in an ice bath prior to the respective addition of aluminum in the form of $C_2H_5CH(CH_3)O)_3Al$ (Aldrich) and titanium in the form of $Ti(OC_2H_5)_4$ (Aldrich). Finally, H_2O (1 mL) was added, and the mixture was allowed to condense for 20 h. In the case of the 1:1 Si:Ti solution, all the water was added to the mixture prior to the addition of the titanium precursor, as unreacted $Ti(OC_2H_5)_4$ in the concentrated mixture immediately condensed as a white precipitate on water addition. The as-formed sol−gel solutions outlined in Table 1 were homogeneous, colorless, and optically transparent for all compositions. The titanosilicate sol−gel solutions were found to be stable for 2−3 months, whereas the aluminosilicate solutions were stable for 1−2 months at ambient conditions.

Fabrication of Highly Ordered Macroporous Films by Dip Coating. The substrate-supported artificial opal was immersed vertically into the alkoxide sol, at a rate of 150 mm min^{-1}, before

(24) Hüsing, N.; Launay, B.; Doshi, D.; Kickelbick, G. *Chem. Mater.* **2002**, *14*, 2429.
(25) Schattka, J. H.; Shvhukin, D. G.; Jia, J.; Antonietti, M.; Caruso, R. A. *Chem. Mater.* **2002**, *14*, 5103.
(26) Fujishima, A.; Rao, T. N.; Tryk, D. A. *J. Photochem. Photobiol. C* **2000**, *1*, 1.
(27) Corma, A.; Martinez, A.; Martinez-Soria, V.; Monton, J. B. *J. Catal.* **1995**, *153*, 25.
(28) Biz, S.; White, M. G. *J. Phys. Chem. B* **1999**, *103*, 8432.
(29) Spirkova, M.; Brus, J.; Hlavata, D.; Kamisova, H.; Matejka, L.; Strachota, A. *J. Appl. Polym. Sci.* **2004**, *92*, 937.
(30) Davis, R. J.; Liu, Z. *Chem. Mater.* **1997**, *9*, 2311.
(31) Ogawa, M.; Ikeue, K.; Anpo, M. *Chem. Mater.* **2001**, *13*, 2900.
(32) Shen, Y.; Wu, Q.-Z.; Liao, J.-F.; Li, Y.-G. *Wuji Cailiao Xuebao* **2003**, *18*, 401.
(33) Gundiah, G. *Bull. Mater. Sci.* **2001**, *24*, 211.
(34) Yoldas, B. *J. Non-Cryst. Solids* **1984**, *63*, 150.
(35) Best, M. F.; Condrate, R. A. *J. Mater. Sci. Lett.* **1985**, *4*, 994.
(36) Schraml-Marth, M.; Walther, K. L.; Wokaun, A.; Handy, B. E.; Baiker, A. *J. Non-Cryst. Solids* **1992**, *143*, 93.
(37) Ryan, K. M.; Erts, D.; Olin, H.; Morris, M. A.; Holmes, J. D. *J. Am. Chem. Soc.* **2003**, *125*, 6284.

Table 1. Molar Compositions of Precursor Chemicals for Mixed Oxide Sol−Gel Solutions: $M_1 = (Ti(OC_2H_5)_4$; $M_2 = (C_2H_5CH(CH_3)O)_3Al$

atomic ratio	$Si(OC_2H_5)_4$	M	HCl	C_2H_5OH	H_2O
(Si:M, 10:1)	0.050	0.005	8×10^{-5}	0.12	0.02
(Si:M, 5:1)	0.050	0.010	8×10^{-5}	0.12	0.02
(Si:M, 3:1)	0.050	0.017	8×10^{-5}	0.12	0.02
(Si:M, 2:1)	0.050	0.025	8×10^{-5}	0.12	0.02
(Si:M. 1:1)	0.025	0.025[a]	8×10^{-5}	0.12	0.02

[a] Only for M = Ti.

immediate withdrawal at 50 mm min^{-1}. The deposition speeds were judiciously selected to allow complete filling of the interstitial voids by capillary action in a single coating. The filled opal was dried at 50 °C for 1 h to support gelation of the inorganic network. Finally, template removal and glass condensation was achieved by heating the sample in air to 350 °C for 30 min at a rate of 2 °C min^{-1}. Residual carbon from the calcination process was removed by placing the sample in an ozone atmosphere for 30 min. Additionally, thickness control of the artificial opal templates was achieved by pre-dilution of the alkoxide sols with ethanol (sol:ethanol, 1:1, 1:2, etc.) prior to dipping. Evaporation of the excess solvent during dip casting and drying resulted in partial filling of the opal template vertically from the substrate. Uncoated spheres were burnt off during calcination leaving a residual porous layer of controlled thickness.

Instrumentation. An analytical scanning electron microscope (JSM-6500F) was used to study both the morphology and microstructure of the macroporous films. A thin layer of gold (20 nm) was evaporated on to the film surface prior to topographical observation and energy-dispersive X-ray (EDX) analysis.

X-ray diffraction (2θ, 10-80) (Siemens D5000) using Cu Kα radiation was used to study the crystallographic structure of both macroporous films and powdered titanosilicate and aluminosilicate samples.

An Olympus BX51 microscope, equipped with a 100-W halogen bulb was used to image the normal incident reflected light off the sample at 10 times magnification. The reflected light is coupled to an Olympus charge-coupled device camera as well as an Ocean Optics "USB 2000" spectrometer to allow simultaneous monitoring of the reflected image and the optical spectra. The spectrometer is fiber coupled and records the spectra from a 50-μm region of the sample from 350 to 1000 nm with an accuracy of 0.3 nm.

The recorded spectra is normalized to the reflectivity of a Spectra Physics aluminum mirror. This removes features in the optical spectra arising from the bulb and other components within the microscope.

Fourier-transform (FT) IR absorption spectra were recorded on a Mattson Satellite FT IR spectrometer fitted with a Specac Golden Gate Single Reflection ATR sampling platform.

The ozone generator was fabricated in the Laboratories at Merck Chemicals, Ltd., Chilworth, Southampton. The generator consisted of a low-pressure grid mercury UV lamp producing short wavelength lines <190 nm suitable for splitting molecular oxygen. The ozone generation occurs very close to the sample surface ensuring maximum penetration of ozone within the macroporous oxides. The samples were exposed to the ozone treatment for 30 min in an extraction hood.

Results and Discussion

Ordered macroporous films were prepared by the sol−gel infiltration of monodisperse (365 nm) close-packed spheres. Figure 1a (I−IV) shows selected scanning electron microscopy (SEM) images of titanosilicate and aluminosilicate macroporous films with M:Si atomic ratios of 1:1, 1:2, 1:4, and 1:5, respectively. The hexagonal arrangement of pores in the inverse opals clearly reflects the close-packed ordering of the colloidal crystal template in each case and is preserved independent of heterometal or loading. Uniformity of thickness in the pore walls further evidences the complete filling of the interstitial voids during sol−gel infiltration. The pore-center to pore-center repeat distance was consistent across the range of Si:M binders and at 329 ± 18 nm reflected a material shrinkage of 10% occurring during calcination. This shrinkage is lower than expected for sol−gel processes (typically 25%) and results in the films cracking into several large domains from 0.1 mm^2 up to 1 mm^2 (Figure 1b). The structural order in the templated macroporous oxides can be realized visually as Bragg diffraction of white light results in vivid diffraction colors, which are dependent on the angle of observation. Figure 1b shows a macroporous sample (2:1, Si:Ti) giving reflections at wavelengths 600−650 nm (orange/red) at normal observation shifting to 550−580 nm (yellow) when illuminated by light at 75° to the observer.

Figure 1c is a further magnified SEM image of a macroporous mixed metal oxide with a binary mixed metal oxide binder consisting of silica and titania in the ratio of 1:1. The in-plane pore diameter is 292 ± 17 nm with an average wall thickness of 37 nm. Again, the in-plane pore diameter was unaffected by titanium content and was constant across the entire range of macroporous mixed metal oxides. Further magnification (Figure 1c) reveals the complicated interconnected network of air spheres in the macroporous framework. Each large cavity in the surface layer contains three internal windows (diameter 50 ± 15 nm) to successive layers at the points of contact of the original spheres. An interesting feature is the presence of small openings, or spandrels (marked with an arrow in Figure 1c, diameter = 5 nm) at the center of each triangular intersection of three air spheres of the top layer of the film. This occurs when the sol condenses on the PMMA sphere blocking the introduction of additional precursor into the intersections.[38]

Thermal shock and shrinkage during calcination are primarily responsible for line defects in the inverse opal structure as observed in Figure 1b. Further defects arise from packing irregularities in the close-packed template. Figure 1d shows a point defect in the inverse opal arising from a missing PMMA sphere in the original template. On average, point defects were limited to one per 150 spheres and were further minimized using slow (several weeks) gravity sediment templates obtained at 3 °C. Analysis of the mixed oxide inverse opals at micron scale resolution reveals regular grain boundaries, typical for sedimented opals, permeating the particles. Figure 1e is a SEM image showing the polycrystalline distribution of the domains in the close packed structure of macroporous (1:1 Ti:Si) titanosilicate. The (111)-oriented domains are on average 55 μm in thickness and are randomly orientated with respect to one another in a striped morphology.

The macroporous pore structure is extremely robust at high temperatures. Figure 1f shows an SEM image of a sample

(38) Zakhidov, A. A.; Baughman, R. H.; Iqbal, Z.; Cui, C.; Ilyas, K.; Dantas, S. O.; Marti, J.; Ralchenko, V. G. *Science* **1998**, *282*, 897.

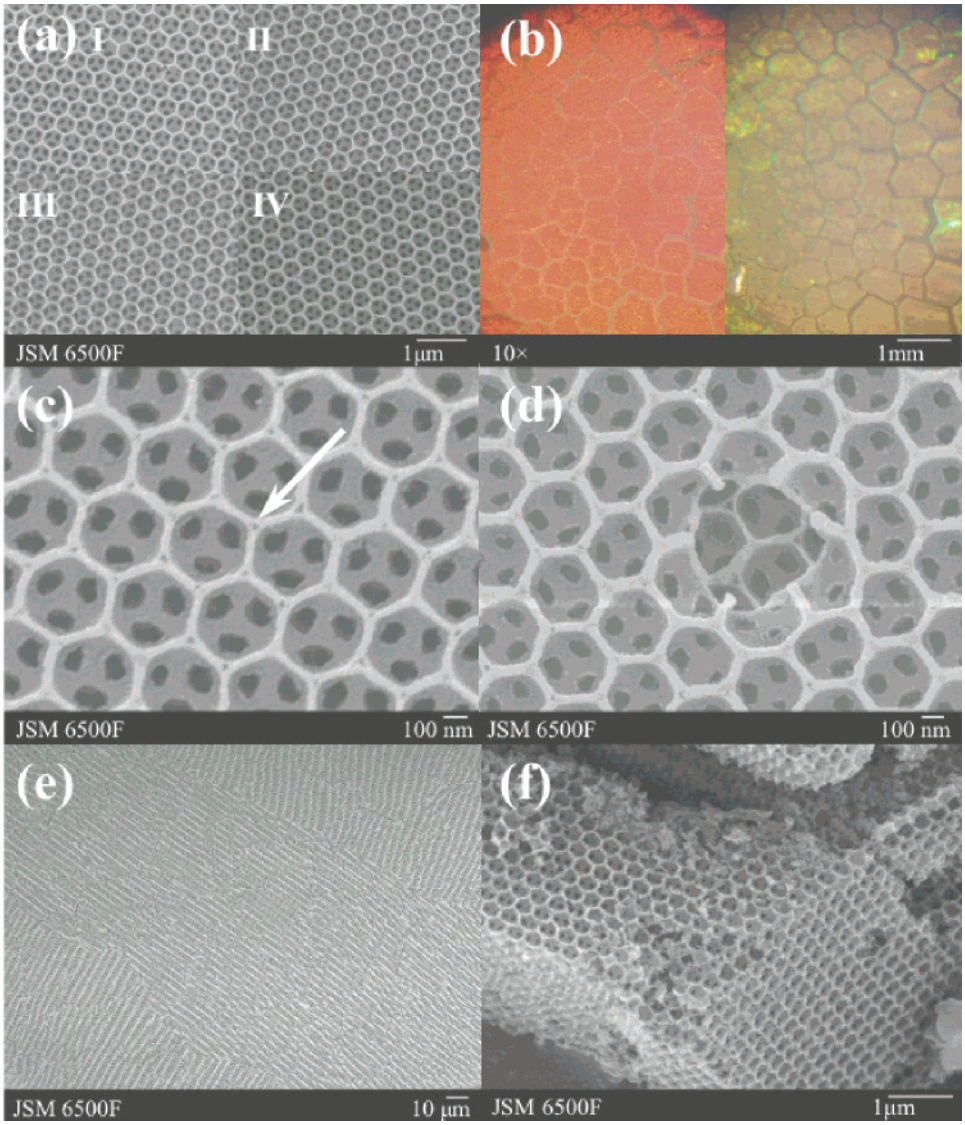

Figure 1. (a) SEM image of macroporous mixed metal oxides with M:Si atomic ratios of (I) 1:1, M = Ti; (II) 1:2, M = Al; (III) 1:4, M = Al; (IV) 1:5, M = Ti. (b) Optical microscope image of macroporous titanosilicate film (Si:Ti, 2:1) illuminated with light at (left) 0° and (right) 75°. (c) SEM image of spandrels in a macroporous titanosilicate sample (Si:Ti, 1:1), (d) SEM image of a point defect in a macroporous titanosilicate sample (Si:Ti, 5:1). (e) SEM image of the polycrystalline nature of a titanosilicate macroporous film, (Si:Ti, 1:1) (f) SEM image of a powdered macroporous titanosilicate sample with a Ti:Si atomic ratio of 1:1 which has been subjected to further heat treatment at 750 °C for 6 h. All images are from samples that were initially calcined at 350 °C to remove the sphere template.

cleaved from a substrate followed by calcination at 750 °C for 6 h. The image is a cross-section of the macroporous network showing that the three-dimensional structure and morphology is preserved at these conditions.

On average, the titanosilicate films were found to be defect free in large domains (10 μm^2) regardless of elemental composition using slow gravity-deposited templates. The even distribution of material at pore walls and smooth topography evidences the uniform deposition of mixed oxide sol−gel precursors during fabrication. Typically, samples were prepared with a thickness of 30 μm (ca. 90 layers) by filling a 30-μm thick artificial opal template from the substrate with the sol−gel solution. The thickness of the inverse opal was adjusted by controlling the extent of void filling in the artificial opals. By use of ethanol-diluted sol−gel solutions of known volume (sol:ethanol: 1:1, 1:2, etc.), artificial opals were partially filled vertically from the substrate as the excess ethanol evaporated. For example, a 40-μm artificial opal filled from the substrate with a solution consisting of 1 part sol and 3 parts ethanol yields a 10-μm film after excess template removal during calcinations. The smallest film thickness obtained by this method was 7 μm (ca. 21 layers). This method of macroporous oxide thickness control compares favorably to that reported by Colvin and co-workers who manipulated parameters such as colloidal concentration and sphere size.[9]

EDX analysis was used to quantify the elemental composition of both the titanosilicate and aluminosilicate matrixes. The EDX data was taken from several areas across the sample, each with a spot size of around 100 nm and as such shows homogeneity over areas with a 100-nm diameter. Figure 2 compares the silicon/titanium and the silicon/aluminum atomic ratios of the calcined macroporous material to the ratio in the initial sol. The silicon/titanium ratio remains constant, whereas the silicon/aluminum ratio deviates very slightly, possibly indicating a slight loss of aluminum in the final film. However, the linear plots obtained are within experimental error of the ideal (dashed diagonal line),

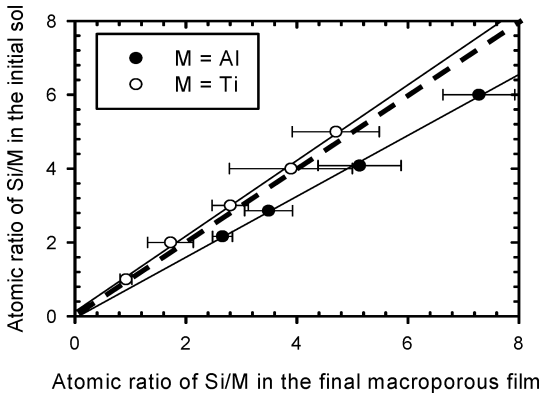

Figure 2. Comparison of the Si/M atomic ratio in the macroporous material to the initial sol concentration for M = Al and Ti (error bars were calculated for 50 measurements, experimental and analysis, by sampling over small areas for 5 samples from distinct batches).

especially at high concentrations, indicating that the ratio of metal to silicon is preserved throughout the deposition and calcination processes. Sol−gel routes toward mixed metal oxides of silicon and aluminum or titanium usually result in precipitation of metal-rich intermediates at the solution stage. Clearly, dimerization and precipitation of titanium-rich or aluminum-rich intermediates has not occurred, as the mixed metal ratio at the pore walls is consistent with reactant concentrations especially for Si:M in 1:1 atomic ratios. The effectiveness of the prehydrolysis route in the formation of homogeneous sols was analyzed in detail using magic-angle spinning NMR in a recent publication by Ryan and co-workers.[36] Briefly, judicious prehydrolysis of silicon alkoxides produces reaction intermediates that react faster with metal alkoxides (M = Al, Ti) than the self-condensation of silicon alkoxide occurs. Ideally, the hydrolysis of the silicon alkoxide in the form of tetraethyl orthosilicate is limited to T^2 ($Si(OH)_2(OEt)_2$), T^3 ($Si(OH)(OEt)_3$), or T^4 ($Si(OEt)_4$) species prior to the addition of heterometal alkoxides. The optimal conditions for this process are 10 min reaction at 40 °C beyond which self-condensed Q^1 ($(OSi)Si(OH)_3$) and Q^2 ($(OSi)_2Si(OH)_2$) species dominate. The optimized prehydrolysis process was highly effective for the formation of Si:Ti binders with a 1:1 atomic ratio and Si:Al in a 2:1 ratio. EDX analysis also revealed significant quantities of residual carbon as a byproduct of template combustion. The carbon content is a potential contaminant in catalytic and optical applications and was removed by passing an ozone stream over the sample for 30 min.

Solid-phase Si−Ti mixed oxides are often characterized by IR absorption spectroscopy. Distinctive absorptions by silica and titania species in the low-wavenumber region of the IR absorption spectrum are particularly useful for characterizing the bonding in titanosilicate materials. Figure 4 shows accumulated spectra for solid-phase macroporous Ti−Si mixed oxides with atomic ratios of 1:1, 1:2, 1:3, 1:4, and 1:10, respectively. The sample with the highest silica loading (Ti:Si, 1:10) selectively absorbs at 800, 920, and 1050 cm^{-1} with a small shoulder at 1200 cm^{-1} related to the longitudinal optical component of the Si−O−Si asymmetric stretching.[39] The lowest wavenumber absorption

(39) Almeida, R. M.; Pantano, C. G. *J. Appl. Phys.* **1990**, *68*, 4225.

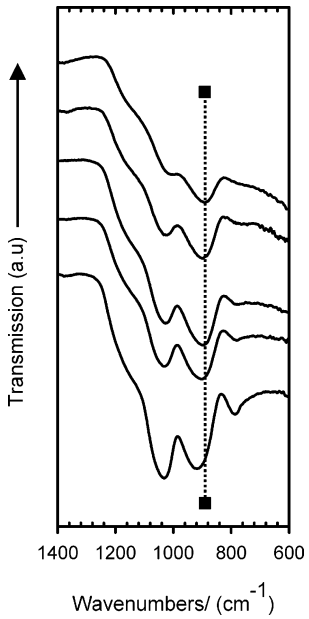

Figure 3. Low-wavenumber FT IR transmission spectra of Si:Ti mixed oxides. (Dashed line is eye guide for peak shifts.)

corresponds to symmetric stretching vibration of Q^4 (SiO_4^{4-}) species. This feature diminishes as more titanium is introduced into the silica framework and is completely absent in macroporous oxides with a 50% titania loading. Similarly, the intensity of asymmetric vibrations from the Q^4 species (1050 cm^{-1}) decreases in line with titanium enrichment. The absorption band at 920 cm^{-1} mirrors that expected for asymmetric stretching of oxygen atoms coordinated to silicon and titanium and is characteristic of homogeneous titanosilicate glasses.[30] Absorption bands in this region can be attributed to the stretching vibrations of the silanol Si−OH groups. However, the constant feature intensity as a function of titania, together with the lack of a further silanol band at 3400 cm^{-1} implies Si−O−Ti is the more likely absorber. Close inspection of the peak at 1050 cm^{-1} shows that the band gradually broadens and shifts to lower frequency as the Si:Ti ratio increases. This behavior can be attributed to successive incorporation of Ti^{4+} ions into the silica network, accompanied by a reduction of the average bond strength of the Si−O bonds in the glass structure.[35] The absence of silica features in the binary (1:1) Si−Ti Macroporous oxide combined with a strong resonance from Si−O−Ti further supports the homogeneous distribution of silicon and titanium atoms in the sol−gel binder after calcination. Clearly, the expected metal leaching has not occurred such that the sol−gel approach is proven effective for the deposition of homogeneous titanosilicate matrixes with 50% loading without the need for complexing agents.

The stability of the mixed metal macroporous oxides as a function of temperature was studied using powder X-ray diffraction (XRD). Figure 4a shows stacked X-ray diffractograms of powdered 1:1 Si:Ti subjected to calcination temperatures from 350 to 1300 °C. As expected, the sol−gel-deposited Si−Ti framework is completely amorphous at 350 °C. The onset of crystallization (950 °C) coincides with an observed loss of opalescence in the corresponding macroporous films as framework degradation leads to macropore collapse (The regular ordering of the macroporous

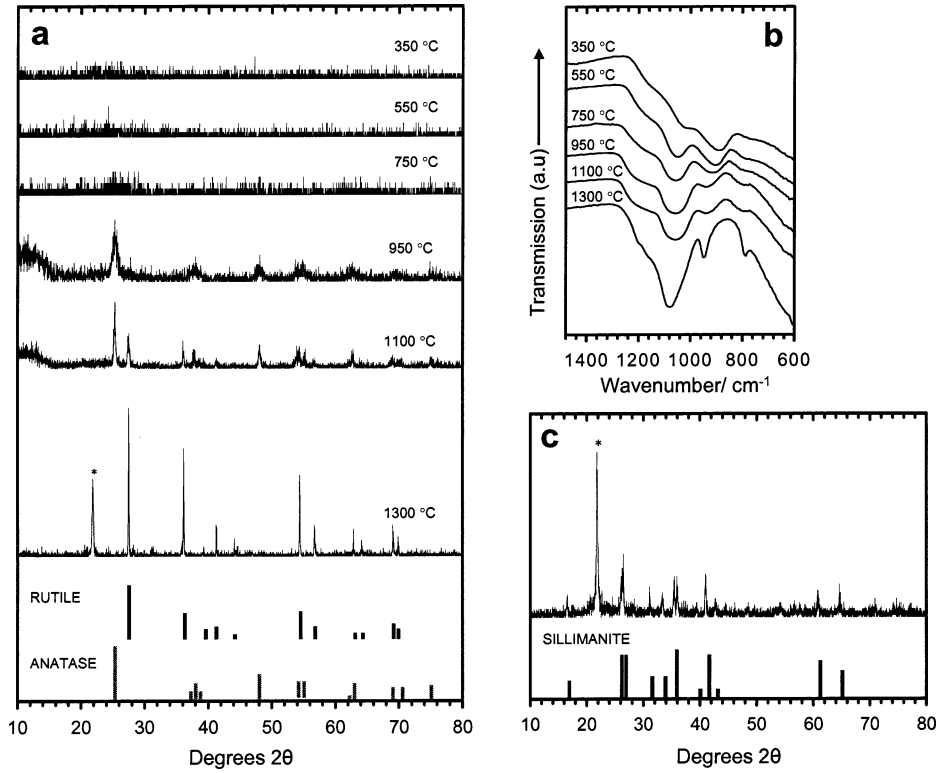

Figure 4. (a) Powder XRD patterns of 1:1 Ti:Si titanosilicate samples calcined at temperature ranges from 350 to 1300 °C. (b) Low-wavenumber FT IR transmission spectra of 1:1 titanosilicate samples calcined at temperature ranges from 350 to 1300 °C. (c) Powder XRD pattern of a 1:2, Al:Si aluminosilicate sample calcined at 1300 °C. The asterisk denotes the crystoballite reflection.

oxides is clearly visible at 750 °C, Figure 1f). Crystalline anatase peaks emerged at 950 °C and sharpened at 1100 °C from particle sintering. At temperature extremes >1300 °C, the rutile phase of TiO_2 dominates and SiO_2 begins to crystallize in the form of crystoballite (Figure 4a).

The macroporous aluminosilicate matrixes were more robust, with pore collapse occurring at 1100 °C. The aluminosilicate (1:2) matrix was completely amorphous up to temperatures of 1300 °C where crystalline reflections from the silica-rich crystoballite phase and the aluminum silicate sillimanite phase (Al_2SiO_5) emerged and sharpened due to sintering at 1300 °C (Figure 4C).

Figure 4b shows accumulated FT IR spectra of a 1:1 titanosilicate matrix calcined at temperatures of (350, 550, 750, 950, 1100, and 1300 °C respectively). The Ti−O−Si absorbance at 920 cm^{-1} is clearly evident at 350 and 550 °C but diminishes considerably as the degree of heterogeneous bonding decreases at greater temperatures. The increase in intensity of the band at 1050 cm^{-1}, resulting from homogeneous Si−O−Si bonding, shows that as the calcination temperature is increased TiO_6-rich phases are formed at the expense of Ti^{4+} in tetrahedral coordination. It is likely that nanosized titanium-rich phases are present even at the lowest temperatures, but prolonged heat treatment causes these regions to grow and eventually crystallize out at sufficiently intense temperatures. The degree of heterogeneous bonding within the titanosilicate matrix is clearly highly dependent upon the temperature at which the samples are treated upon template removal.

Reflectance spectra were recorded for macroporous mixed oxide samples at normal incidence in the range 400−1000 nm. Figure 5 shows the reflectance spectra of titanosilicate films with Ti:Si ratios of 1:1, 1:4, and 1:10, respectively. A large diffraction maximum is observed at around 610 nm, and this maximum clearly shifts toward higher wavelengths with increasing titanium incorporation.

The effective refractive index of the film (n_a) can be evaluated using the Bragg equation (eq 1) where λ is the maximum of the reflectance peak, d is the lattice constant, n_a is the average refractive index of the film, and θ is the angle of incident light. As the dominant surface in our fcc samples is the (111) face, d can be evaluated by eq 2, which gives the relationship between the lattice constant (d) and nearest neighbor distance of spheres (D). Finally the refractive index of the titanosilicate material (n_0) can be evaluated by eq 3, where n_{air} is the refractive index of air, which is 1, and ϕ is the volume fraction occupied by the air spheres, which is 0.74 for inverse opaline structures.

$$\lambda = 2dn_a \sin\theta \tag{1}$$

$$d = d_{111} = (2/3)^{1/2}D \tag{2}$$

$$n_0 = (n_a - n_{air}\,\phi)/(1 - \phi) \tag{3}$$

The refractive indexes of the mixed macroporous oxides as a function of atomic ratios were calculated with $D = 329$ nm (constant for all the samples) and a volume fraction, $\phi = 0.74$, typical for hexagonal close packing. The refractive indexes are shown in Table 2 and range between 1.526 and 1.625. These values show incremental increases from a pure silicate sample synthesized in the same manner ($n = 1.431$) as a function of titania incorporation. Therefore,

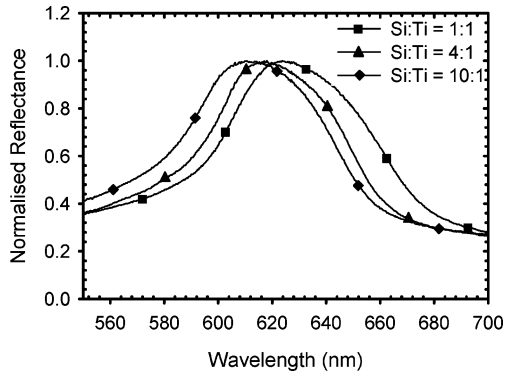

Figure 5. Optical reflectance spectra of Si:Ti mixed oxides.

Table 2. Atomic Ratios, Reflection Wavelength Maximas, and Refractive Indexes of a Range of Titanosilicate Macroporous Oxides

atomic ratio Si/Ti	peak maxima (nm)	n_a	n_0
1	624.5	1.163	1.625
2	622.1	1.160	1.614
3	619.7	1.156	1.601
4	618.0	1.151	1.579
5	616.7	1.149	1.572
10	610.3	1.137	1.527

the incorporation of titania in silicate networks using prehydrolysis-assisted sol−gel routes allows the effective modulation of refractive index as a function of Si:Ti atomic ratio.

Conclusion

The formation of three-dimensionally ordered macroporous mixed metal oxides using a facile sol−gel process is reported. Judicious prehydrolysis of the silicon alkoxide precursors allows the formation of titanosilicate and aluminosilicate macroporous oxides with very high heterometal loading. In particular, the route allows macroporous oxides to be synthesized with framework walls consisting of Si:Ti oxide walls in a 1:1 ratio. The titanosilicate and aluminosilicate porous networks were stable to temperature extremes of 800 and 1000 °C, respectively, prior to crystalline phase separation and pore collapse. Consequently, the mixed macroporous oxides are ideal for high-temperature catalytic applications with large molecular weight compounds. This work represents a significant advance in the synthesis of mixed metal oxide macroporous oxides where previous synthetic routes were limited to a maximum of 3:1 silica:heterometal loading and required the use of complexing agents to equalize the hydrolysis rates of the metal alkoxide precursors. The ability to vary the heterometal content with precision allowed the refractive index of the macroporous matrix to be effectively modulated. Controlling the refractive index of a material periodic to the wavelength of light has useful applications for light manipulation in photonic systems.

Acknowledgment. The authors would like to thank Barbara Cressey and Shuncai Wang of the Electron Microscopy Centre in the Southampton University Chemistry department and Tim Kelf of the Jeremy Baumberg group from the Southampton University Physics department for assistance with the reflectance spectra. Steven Hant acknowledges the support of the EPSRC and Merck Chemicals, Ltd., for Cooperative Awards in Science and Engineering funding. Industrial Host Fellowship funding for Kevin Ryan under the European 5th Framework Marie Curie initiative is also acknowledged.

CM0482582